THERMALLY-DRIVEN SNAP-THROUGH AND MULTISTABILITY USING LAMINATED FIBRE-METAL SHELLS

E. Eckstein*, E. Lamacchia, A. Pirrera, P. M. Weaver

Advanced Composites Centre for Innovation and Science, University of Bristol, Queen's Building, Bristol BS8 1TR, United Kingdom
* *Corresponding Author: eric.eckstein@bristol.ac.uk*

Keywords: thermal actuation, morphing, multistability, hybrid laminate,

Abstract
Fibre-metal laminated shells possessing initial cylindrical curvature are and experimentally tested. These shells display thermally-driven snap-through behaviour, that is, they abruptly snap to new shapes by sole application of thermal loading. Additionally, the shells display deadband hysteretic behaviour, snapping at different temperatures depending on whether they are heated or cooled. This behaviour is broadly similar to several existing approaches towards thermal snap-through, however the physical mechanism utilized herein is distinctly different. This fact, combined with the use of composite materials, yields a concept which is free from the extensive geometric limitations of current thermal snap-through approaches, and thus may be potentially useful in morphing and fluid control applications. Experimental results are compared to two contemporary analytical multistability models as well as a finite element model.

1. Introduction

Thermally actuated structures are defined by their ability to exhibit a shape change in response to temperature change. This shape change can be driven by thermal expansion, or to be more specific, the associated driving stresses can be generated by thermal expansion coefficient (CTE) mismatch between two or more materials. Other methods of thermal actuation have been explored, including shape memory materials and phase-change systems, however the aforementioned CTE-mismatch strategy forms the basis of this study.

Work can be extracted from CTE-mismatch structures using a bimorph mechanism, whereby two or more constituent materials are joined in a laminate such that each material's thermally induced tensile and compressive stresses act remote from the neutral axis, thus generating a bending moment. This behaviour is observed in the common bimetal strip, and has found applications in thermostats, circuit breakers, and spacecraft passive thermal management systems. The use of isotropic materials, however, limits the acceptable range of actuator geometries available to the designer. Mansfield has shown that because the bending stiffnesses and thermal moments are equal in all directions for such a laminate, the energetically preferable direction of bending is determined by the laminate's geometry [1], and thus 1-dimensional bending actuation in a targeted direction is only achievable using slender, strip-like structures. Bending deformation perpendicular to the structure's long axis, such as that required for a trailing edge

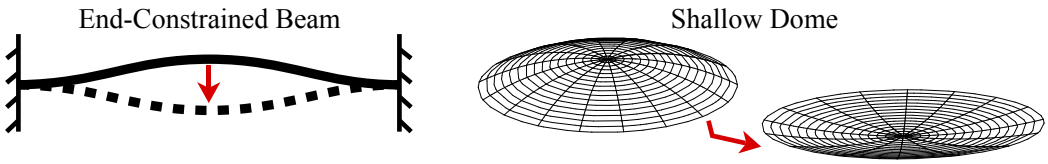

Figure 1. Basic geometries utilized for achieving nonlinear temperature response with isotropic materials.

airfoil control surface, would be untenable without the use of directional stiffening mechanisms such as stringers or corrugations. The use of composite materials opens the possibility to create thermal actuators which are anisotropic in terms of both stiffness and thermal moments. The direct result of this is that bimorph actuators may be created which exhibit bending action in a direction determined by material orientations, thus allowing the designer freedom to specify general planform geometries.

Free-standing thermal bimorph beams exhibit approximately linear bending response to temperature change, yet for many applications, the designer may instead which to specify a highly nonlinear response, such as displacement concentrated within a temperature window, or perhaps even a step-change response. This is currently achievable with isotropic bimorphs using various permutations of either the end-constrained beam or shallow dome approaches [2], as illustrated in Fig. 1. While the effectiveness and reliability of these mechanisms has been proven in circuit breaker and thermostat applications, their limited geometrical design space restricts them from general actuation and morphing applications, particularly where the actuator skin is to be employed as an aerodynamic surface.

We seek to demonstrate that the tailorability of composite materials, combined with the geometrically nonlinear large-displacement response of thin shells, can yield thermal bimorph actuators with highly nonlinear displacement response to temperature change. Step-change displacement response, snap-through, and even multistability become possible. No fixed end-constraints are necessary, allowing for the sort of cantilevered implementations that would be required for trailing edge aerodynamic surfaces. Additionally, a much greater variety of planform geometries are feasible than what is possible with isotropic materials.

2. Mechanics

2.1. Exploiting Geometric Nonlinearity of Thin Shells

Although a nonlinear response to temperature change can be achieved with certain smart materials, we seek to demonstrate that such behaviour can also be attained using conventional engineering materials. As thermal stresses tend to scale approximately linearly with temperature for most structural materials, significantly nonlinear response must instead be achieved via exploitation of geometric nonlinearity, or in other words, by designing a structure whose stiffness is highly dependent upon shape. Thin shells with initial curvature display such behaviour when loaded with bending moments perpendicular to the initial curvature direction [3]. Consider the shell shown in Fig. 2, with an applied internal bending moment (perhaps from thermal loading) along the x-direction, M_x^{th}. From a beam-mechanics perspective, the effective bending stiffness of the structure as a whole along this direction is a function of not only the laminate's $\boldsymbol{D}$-matrix terms from classical lamination theory, but also the geometric stiffness granted by

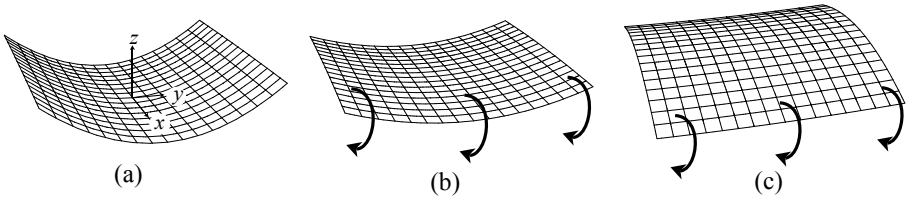

Figure 2. Response of curved shell to applied internal bending moment perpendicular to initial curvature direction.

the curvature in the y-direction. This stiffens the plate in the same manner that an extended carpenter's tape measure is stiffened by its transverse curvature. Alternatively, one can view the problem from a shell mechanics perspective, whereby a singly-curved surface will initially resist development of Gaussian curvature through storage of membrane strain energy. When M_x^{th} exceeds some critical value, it becomes energetically favorable for thin-walled structures to instead accommodate load with bending strain energy, manifested by curvature generation in the x-direction. As shown in Fig. 2b-c, this increase in κ_x is accompanied by of loss of κ_y as required to minimize Gaussian curvature and its associated membrane strain energy. Returning to the beam perspective, the geometric bending stiffness granted by transverse curvature is lost upon Brazier collapse [4] of the section to a flat strip, allowing the beam to deform in the direction of moment application. This behaviour can be observed by bending an everyday carpenter's tape measure.

2.2. Generation of Internal Moments

Generation of thermal stress requires selection of lamina possessing mismatched CTEs. In particular, actuation forces are maximized by selecting high modulus materials with greatest possible CTE mismatch [2]. Unidirectional (UD) carbon-epoxy composite fulfills the role of the low-expansion element. It possesses a near-zero CTE in the fibre direction, but is highly anisotropic, thus allowing for the direction of primary bending moment to be closely controlled. While the high-expansion element can also be of composite construction by utilizing the relatively high α_2 of carbon-epoxy lamina as achieved with unsymmetric (e.g. [0/90] laminates), Daynes and Weaver [5] demonstrated that fibre-metal hybrid laminates yielded superior thermal moments relative to all-composite unsymmetric laminates on account of the superior modulus of engineering alloys relative to E_2 of carbon-epoxy UD lamina. For this study, we have selected 5251-H22 aluminium alloy as our high-expansion element on the basis of its relatively high CTE and widespread availability.

3. Modelling Methodology

Researchers in the field of multistable structures have produced a host of analytical models aimed at predicting the large-displacement response of initially curved shells to internal moments, and thus these models form the basis of our analysis. In this study, we utilize the work of Refs. [6] and [7] to analytically model the response of a composite thermal actuator. The former model fully accounts for temperature-dependent material properties continuously with respect to temperature. The latter model has been solved at 30°C increments, with the corresponding material properties updated at each increment; thus temperature dependent properties are still accounted for, albeit in an incremental manner.

Layup	[metal/composite]	$[Al_1/0_4^\circ]$
Al sheet thickness	[mm]	1.20
AS7/M21 UD ply thickness	[mm]	0.286
Side Lengths L_x, L_y	[mm]	230
x-direction tool curvature	[mm^{-1}]	0
y-direction tool curvature	[mm^{-1}]	$-1/400$

Table 1. Test article manufacturing parameters.

The model presented in Ref. [7] is an energy based approach to describe the stability of doubly curved shells of elliptical planform. Vidoli decoupled the membrane and a bending components of total potential energy, then used the in-plane equilibrium equations and the compatibility conditions between in-plane strains and curvatures (Gauss Theorema Egregium) to express the membrane component of the shell's total potential energy in terms of curvatures only. By so doing, the membrane equilibrium can be solved separately using a finite element model. The shell's stable equilibria are then obtained by minimizing the total potential energy with respect to the curvatures. Using a similar approach, we solve the membrane problem using the differential quadrature method [8]. In this work, we use Legendre polynomials to express the out-of-plane displacements. This approach brought several improvements in the model, especially regarding the description of the deformed shapes and their boundary layers.

A finite element (FE) benchmark model was created using ABAQUS 6.12 with a mesh of 256 S8R quadratic shell elements. Because the structure under investigation displays negative stiffness upon snap-through, the conventional iterative nonlinear solution techniques classically used for multistability analysis [9] fail to converge. Although these solutions can be stabilized using artificial damping techniques, we found that in practice, the resulting displacements were highly sensitive to the degree of damping applied, and convergence of displacements for incremental reductions in artificial damping could not be achieve before solution stability was compromised. Thus, we instead adopted an arc-length solution technique, as implemented in ABAQUS as the Riks method. Solution convergence was verified on the basis of both displacements and snap-through temperatures in terms of both mesh density and arc length time step.

4. Experimental Technique

A laminated fibre-metal shell was constructed to the specifications in Table 1. The aluminium panel was roll-formed along the grain direction to match the tool radius 400 mm. The bond surface was roughened with 200 grit sandpaper, then washed with acetone. The aluminium and unidirectional prepreg were bonded during the autoclave cure cycle using the native prepreg resin, i.e., no interlayer adhesive was utilized. The cure cycle was modified from its manufacturer-specified form in that pressure was released before cool-down, as opposed to the conventional post-cooling pressure release. This change prevents the cured part from being constrained to the shape of the tool during the cool-down process, thus reducing thermal stresses. Despite this precaution, some matrix cracking was observed in the finished part.

After trimming to size, a 6 mm hole was drilled in the center of the plate, through which a single screw joined the laminate to a dial gauge rig via a post, as shown in Fig. 3. The rig

Figure 3. Test article mounted on dial gauge rig. Note that the speckle pattern visible is not relevant to this particular experiment.

	Hexcel AS7/M21 UD						Al 5251-H22		
Temp.	E_1	E_2	G_{12}	ν_{12}	α_1	α_2	E	ν	α
[°C]	[GPa]	[GPa]	[GPa]	[-]	$[\frac{10^{-6}}{°C}]$	$[\frac{10^{-6}}{°C}]$	[GPa]	[-]	$[\frac{10^{-6}}{°C}]$
30	129.55	8.85	5.28	0.33	-2.3	23.4	72.0	0.33	23.0
60	127.99	8.42	4.88	0.33	-2.1	27.8	71.3	0.33	23.0
90	127.47	7.92	4.65	0.33	-1.5	28.6	70.6	0.33	23.0
120	127.18	7.57	4.50	0.33	-0.5	30.0	69.8	0.33	23.2
150	126.11	7.18	4.26	0.33	1.7	32.1	68.4	0.33	23.4
170	125.58	6.76	4.01	0.33	2.6	33.5	67.7	0.33	23.6
180	125.31	6.48	3.77	0.33	2.3	33.5	67.0	0.33	23.6

Table 2. Thermoelastic material data for AS7/M21 UD composite and 5251-H22 aluminium alloy. Thermal expansion coefficients use a reference temperature of 20°C.

consisted of a steel bed, to which an array of four dial gauges were mounted so as to measure transverse displacement at a point along 0°, 90°, and ±45° paths from the laminate's centerpoint. In order to minimize the laminate's distortion due to contact forces from the dial gauge probes, the gauges' internal return springs were removed, thus the weight of the probe itself was the sole contributor of contact force. Graphite lubricant was applied at each probe contact point to minimize measurement error due to friction. Curvature components κ_x and κ_y were found by determining the radii of circular arcs constrained to be tangent to the laminate centerpoint while passing through the point where the respective 0° and 90° dial gauges made contact. Twist curvature κ_{xy} was computed from the difference in displacements along the ±45° paths, and was found to be negligible throughout the experiment, thus it will be henceforth neglected. The laminate was heated by placing the complete dial gauge assembly in an oven and ramping the temperature up to 180°C at a rate of 1°C/min, followed by an equivalent-rate cool-down to 20°C. Temperature was measured using a thermocouple adhered to the laminate with the aid of thermally conductive paste.

Temperature-dependent material data for Hexel AS7/M21 UD prepreg was obtained by experiment as detailed in Ref. [6], and is reproduced in Table 2. Material data for 5251-H22 aluminium alloy was sourced from Ref. [10], and is also contained in Table 2. Where data at intermediate temperature values was unavailable, data from similar alloys was utilized to aid interpolation.

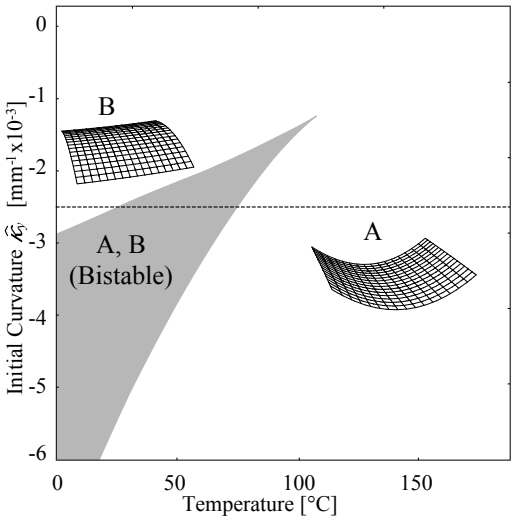

Figure 4. Stability diagram showing potential laminate shapes for a range of initial curvatures and temperatures for the layup given in Table 1. The dotted line represents the initial curvature of the experimentally tested laminate.

5. Results

The model from Ref. [6] was used to plot the predicted shape and stability landscape of the stacking sequence described within Table 1 across a range of temperatures and initial curvatures, as shown in Fig. 4. The model predicts that the thermal snap-through process consists of an inversion of major curvature sign, and an orthogonal shift in major curvature orientation, similar to the classic shape change exhibited by unsymmetric bistable laminates as detailed in Ref. [11]. For a given initial curvature, the predicted temperature of snap-through depends on whether the structure is being heated or cooled, with the heating snap-through occurring at a higher temperature than the cooling snap-through. Between these two critical temperatures exists a window within which the laminate is bistable. These behaviours are similar to the deadband hysteresis displayed by end-constrained bimorph beams as installed in anti-chatter thermostats. There also exists a minimum initial curvature magnitude required for the laminate to take on snap-through behaviour, below which the structure will instead undergo a smooth shape transition through a saddle shape.

Results from experiment are compared with model predictions for the shell described in Table 1, and are shown in Fig. 5. The experimental results show curvatures as measured during both heating and cooling cycles. The window of bistability predicted by the models is qualitatively replicated by experiment, however there exists significant error in prediction of the snap-through temperatures. Given that the models are in general agreement with each-other, a likely source of error is the existence of any non-thermoelastic strains, which are presently not accounted for in our analysis. Daynes and Weaver [5] observed significant non-thermoelastic strains in their coverage of bistable plates incorporating metal layers, and attributed these strains to slippage between the fibrous and metallic layers during the cure process. It is also possible that the matrix cracking mentioned in Section 4 has led to localized relaxation of thermal moment M_y^{th}. This would have the knock-on effect of allowing κ_y to be suppressed more easily by the primary thermal moment M_x^{th}, thus leading to premature transition to a κ_x-dominated shape upon cool-down. Other potential sources include tool-part interactions [12, 13] and resin shrinkage [14].

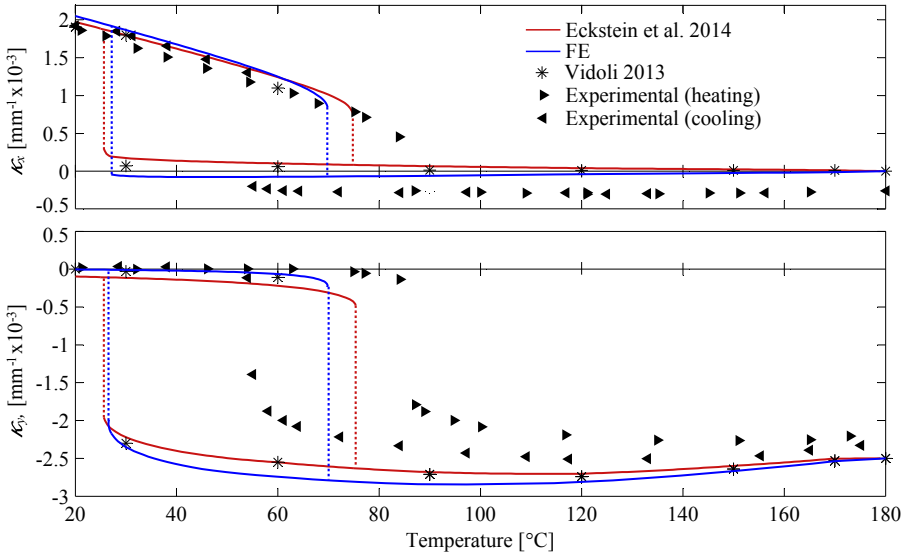

Figure 5. Curvature diagram showing the laminate's nonlinear response to temperature change. Dotted lines indicate snap-through paths. The laminate's predicted bistability window lies between the dotted lines for each set of results. Unstable branches predicted by the models are omitted for clarity.

The experiments also confirm the deadband hysteresis behaviour predicted when cycling across and beyond the range of the bistability temperature window. Further investigation using mechanical forcing confirmed that the laminate was in fact bistable between the two snap-through temperatures. While the experimentally measured heating and cooling curves are nearly identical at temperatures below the bistability window, they differ significantly above the window. Modelling results do not predict this apparently hysteretic behaviour, and although matrix plasticity is suspected, we cannot verify a definitive cause at this time. Further investigation will be required to determine whether this observed behaviour is consistent under additional thermal cycling.

6. Conclusion

A concept for achieving thermally driven snap-through behaviour has been experimentally demonstrated using a fibre-metal laminate. This is achieved by orienting unidirectional, low-expansion carbon fibres perpendicular to the direction of initial curvature. With sufficient stress-free initial curvature, the transition from one cylindrical shape to its orthogonal conjugate occurs in an unstable, non-smooth manner. In addition to the observed snap-through behaviour, a temperature-curvature relationship was achieved such that the laminate was nearly inert upon cool-down from cure temperature, up until the cooling snap-through temperature was approached. This result could potentially be useful for applications whereby the designer wishes to concentrate a thermal actuator's displacement within a small temperature window. Additionally, deadband hysteresis behaviour was observed, with the laminate also demonstrating bistability between the two snap-through temperatures. Two analytical models as well as a finite element model were compared, and although the models predicted similar results to each-other, all significantly underpredicted the snap-through temperatures. This is attributed to the presence of non-thermoelastic strains, which are not presently accounted for in the analysis.

References

[1] E. H Mansfield. Bending, buckling and curling of a heated elliptical plate. *Proceedings of the Royal Society of London. Series A. Mathematical and Physical Sciences*, 288(1414):396–417, November 1965.

[2] S. Timoshenko. Analysis of bi-metal thermostats. *J. Opt. Soc. Am*, 11(3), 1925.

[3] M. W. Hyer and P. C. Bhavani. Suppression of anticlastic curvature in isotropic and composite plates. *International Journal of Solids and Structures*, 20(6):553–570, 1984.

[4] L. G. Brazier. On the flexure of thin cylindrical shells and other thin sections. *Proceedings of the Royal Society of London. Series A*, 116(773):104–114, 1927.

[5] Stephen Daynes and Paul Weaver. Analysis of unsymmetric cfrp-metal hybrid laminates for use in adaptive structures. *Composites Part A: Applied Science and Manufacturing*, 41(11):1712–1718, November 2010.

[6] E. Eckstein, A. Pirrera, and P.M. Weaver. Multi-mode morphing using initially curved composite plates. *Composite Structures*, 109:240–245, March 2014.

[7] Stefano Vidoli. Discrete approximations of the foppl-von karman shell model: From coarse to more refined models. *International Journal of Solids and Structures*, 50(9):1241–1252, May 2013.

[8] H. Du, M. K. Lim, and R. M. Lin. Application of generalized differential quadrature method to structural problems. *International Journal for Numerical Methods in Engineering*, 37(11):1881–1896, June 1994.

[9] M. Schlecht, K. Schulte, and M.W. Hyer. Advanced calculation of the room-temperature shapes of thin unsymmetric composite laminates. *Composite Structures*, 32(1-4):627–633, 1995.

[10] *ESDU Metallic Materials Data Handbook, Section 6: Aluminium Alloys*. IHS ESDU, supplement 47 edition, July 2012.

[11] Michael Hyer. Some observations on the cured shape of thin unsymmetric laminates. *Journal of Composite Materials*, 15(2):175 –194, March 1981.

[12] M Gigliotti, M.R Wisnom, and K.D Potter. Development of curvature during the cure of AS4/8552 [0/90] unsymmetric composite plates. *Composites Science and Technology*, 63(2):187–197, February 2003.

[13] Maenghyo Cho and Hee Yuel Roh. Non-linear analysis of the curved shapes of unsymmetric laminates accounting for slippage effects. *Composites Science and Technology*, 63(15):2265–2275, November 2003.

[14] D. W. Radford and T. S. Rennick. Separating sources of manufacturing distortion in laminated composites. *Journal of Reinforced Plastics and Composites*, 19(8):621–641, May 2000.